JOURNAL OF SOLID STATE CHEMISTRY 113, 27–36 (1994)

Topotactic Oxidation of Ramsdellite-Type $Li_{0.5}TiO_2$, a New Polymorph of Titanium Dioxide: TiO_2(R)

J. Akimoto,[1] Y. Gotoh, Y. Oosawa, N. Nonose, T. Kumagai, and K. Aoki

National Institute of Materials and Chemical Research, Higashi, Tsukuba, Ibaraki 305, Japan

and

H. Takei

Institute for Solid State Physics, University of Tokyo, Roppongi, Minato-ku, Tokyo 106, Japan

Received June 10, 1993; in revised form January 10, 1994; accepted January 12, 1994

The topotactic oxidation in air at room temperature of the lithium titanate bronze Li_xTiO_2 ($x = 0.5$) crystals with the ramsdellite-type structure leads to lower x values and decreased unit-cell volumes. The crystal structures of the three specimens, $Li_{0.41}TiO_2$, $Li_{0.16}TiO_2$, and $Li_{0.14}TiO_2$, have been determined by the single-crystal X-ray diffraction method. The deintercalation of lithium in Li_xTiO_2 with $0 \leq x \leq 0.5$ has been investigated by difference-Fourier maps at $z = 1/4$ sections. The complete oxidation of parent bronze crystals using an acidic solution obtained colorless crystals of a new polymorph of titanium dioxide, TiO_2(R). It crystallizes in the orthorhombic ramsdellite-type structure, in the same space group *Pbnm* with $a = 4.9022(14)$ Å, $b = 9.4590(12)$ Å, $c = 2.9585(14)$ Å, $V = 137.18(7)$ Å^3, $D_x = 3.87$ g/cm^3. $D_m = 3.80$ g/cm^3, and $Z = 4$. The TiO_2(R) structure was also refined from the single-crystal X-ray study to the conventional values $R = 0.049$ and $wR = 0.044$ for 596 independent reflections. When heated above 640 K, TiO_2(R) transforms into brookite-type TiO_2. DTA and IR data of TiO_2(R) are measured.

INTRODUCTION

Recent low-temperature synthetic techniques called "chimie douce" can be used to facilitate the formation of new, frequently metastable, materials. By a preparation method using topotactic reactions of the host lattices, two metastable polymorphs of titanium dioxide; TiO_2(B) and TiO_2(H), have been produced. TiO_2(B) (1) has been prepared by hydrolysis of $K_2Ti_4O_9$, followed by heating at 773 K, and has the host framework of the Wadsley bronze Na_xTiO_2 with $0.20 < x < 0.25$ (2). This phase has been recently found in natural anatase crystals as intergrown lamellae (3, 4). TiO_2(H) (5) has been prepared by the topotactic oxidation of the potassium titanate bronze K_xTiO_2 ($0.13 < x < 0.25$) with the hollandite-type structure.

Recently, we have synthesized single crystals of the lithium titanate bronze $Li_{0.5}TiO_2$ with the ramsdellite (γ-MnO_2)-type tunnel structure and determined their crystal structure (6). The distorted octahedral sites in $Li_{0.5}TiO_2$ are occupied by only Ti atoms, and Li atoms are located at one tetrahedral tunnel site with an occupancy factor of about 50%. In air, the as-grown crystals were very reactive, and a remarkable change in the lattice parameters was observed, together with a decrease in the Li content (6). In this paper, we have examined the topotactic oxidation of the $Li_{0.5}TiO_2$ single crystals, and the crystal structures of four ramsdellite-type Li_xTiO_2 specimens are determined. By complete topotactic oxidation using an acidic solution, single crystals of a new polymorph of titanium dioxide, TiO_2(R), have been prepared.

EXPERIMENTAL AND RESULTS

Topotactic Oxidation

Single crystals of ramsdellite-type $Li_{0.5}TiO_2$ were synthesized by the reaction of lithium metal and titanium dioxide at 1473 K (6). The topotactic oxidation of the as-grown $Li_{0.5}TiO_2$ crystals in air was then carried out. By exposing the as-grown $Li_{0.5}TiO_2$ crystals to air for a few days, for 1 month, and for about 1 year, three Li_xTiO_2 specimens, $Li_{0.41}TiO_2$, $Li_{0.16}TiO_2$, and $Li_{0.14}TiO_2$, each with different lattice parameters, were prepared. The chemical formulae of these oxidized crystals were determined by single-crystal X-ray structure analyses and are used, including $Li_{0.45}TiO_2$, for the as-grown crystal compositions. The oxidation reaction in air using single crystals was not completed, and the most oxidized specimen in this experiment had a chemical formula of $Li_{0.14}TiO_2$

[1] To whom all correspondence should be addressed.

0022-4596/94 $6.00

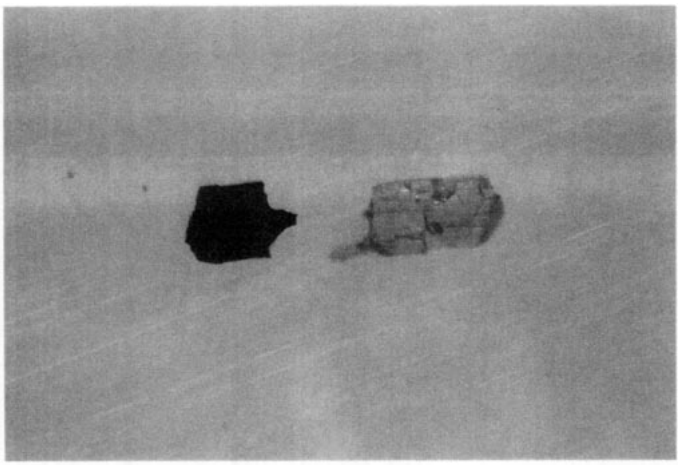

FIG. 1. Single crystals of as-grown $Li_{0.45}TiO_2$ (left) and the final product TiO_2(R) (right).

and was black. We then attempted to prepare completely oxidized crystals using an acidic solution of hydrogen chloride. No stirring or heating was performed. The bubbling of H_2 gas from the surface regions of crystals was observed. After about 10 days of soaking in the solution, the crystals changed from black to light yellow or became colorless. As-grown $Li_{0.45}TiO_2$ and final TiO_2(R) crystals are compared in Fig. 1.

The Ramsdellite Oxide TiO_2(R)

The final TiO_2(R) crystals thus obtained were found to be very stable during the following observations and during single-crystal X-ray diffraction study at room temperature. Figure 2 shows a SEM photograph of the produced

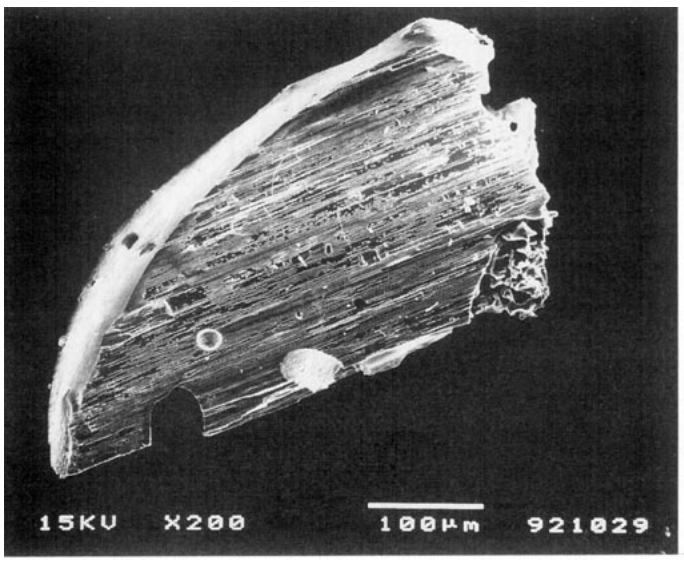

FIG. 2. SEM photograph of a final product TiO_2(R) single crystal.

TABLE 1
X-Ray Powder Diffraction Data for TiO_2(R)

h	k	l	d_{calc}[a] (Å)	d_{obs} (Å)	I/I_0
0	2	0	4.726	4.726	2
1	1	0	4.351	4.346	100
1	2	0	3.402	3.399	3
1	3	0	2.650	2.648	7
1	1	1	2.446	2.446	2
0	4	0	2.363	2.364	2
1	2	1	2.232	2.232	2
2	2	0	2.176	2.176	3
1	3	1	1.974	1.973	1
2	3	0	1.934	1.936	2
2	1	1	1.851	1.850	1
2	2	1	1.753	1.753	1
2	3	1	1.619	1.619	1
3	2	0	1.544	1.544	1
1	5	1	1.515	1.515	10
2	5	0	1.497	1.497	1
3	1	1	1.414	1.414	1
1	1	2	1.400	1.400	1
1	3	2	1.292	1.291	1
0	4	2	1.254	1.254	1
3	4	1	1.223	1.224	1

[a] Refined cell parameters using powder data are a = 4.901(1) Å, b = 9.453(3) Å, c = 2.9580(6) Å, and V = 137.04(3) Å^3.

TiO_2(R) single crystal, whose surface grooves are parallel to the crystallographic c-axis.

Table 1 shows X-ray powder diffraction data of powdered TiO_2(R) crystals obtained at a scan rate of 2°/min in 2θ using graphite-monochromatized Cu$K\alpha_1$ radiation (λ = 1.5406 Å) and a Si internal standard. The typical X-ray powder diffraction pattern is shown in Fig. 3. The lattice parameters of TiO_2(R), determined by a least-squares refinement using powder data, are a = 4.901(1) Å, b = 9.453(3) Å, c = 2.9580(6) Å, and V = 137.04(3) Å^3.

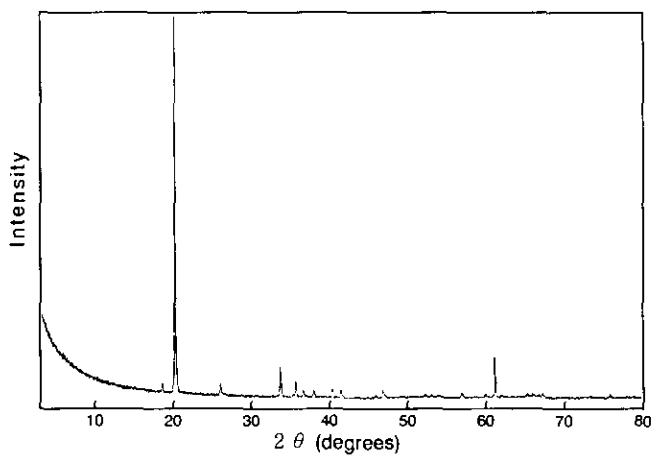

FIG. 3. X-ray powder diffraction pattern of TiO_2(R).

EDX analysis indicates that the only heavy metal component in the oxidized crystals is titanium. Quantitative chemical analysis has been performed using a powdered TiO_2(R) sample (sample weight, 4.72 mg) obtained by picking up and crushing about 30–40 grains of the single-crystal specimens, of average size 0.1 × 0.1 × 0.03 mm. The X-ray powder pattern of this sample showed a few weak peaks that were not indexed to the ramsdellite structure. Further, dark yellow or black impurities on the surface region of the crystals have been observed by microscopic observation. Because it is difficult to remove such impurities, the sample has been analyzed by ICP-MS. The resulting value is 0.78 wt.% lithium, which is thought to result mainly from such impurities.

TGA undergoes no significant weight loss when heated up to 873 K. FT-IR data on a single-crystal specimen (crystal size about 0.1 × 0.1 × 0.04 mm) show no distinct absorption corresponding to the OH stretch vibration between 3000 and 4000 cm^{-1} (Fig. 4). The density of TiO_2(R), measured using the single-crystal specimen and Clerici's heavy fluid, is 3.80 g/cm^3; this value is consistent with the calculated value of 3.87 g/cm^3. These results allow one to conclude that the topotactic oxidation process transforms lithium titanate bronze into a new titanium dioxide, and that the oxide produced is not hydrated.

This new form of titanium dioxide, TiO_2(R), is presumed to be metastable, as are TiO_2(B) (1) and TiO_2(H) (5). DTA (Fig. 5) exhibits two exothermic peaks at 530 and 640 K. An X-ray powder diagram and single-crystal X-ray photographs show that the latter peak corresponds to the transformation of TiO_2(R) into the brookite-type TiO_2. The lattice parameters of brookite thus obtained are a = 5.453(5) Å, b = 9.202(4) Å, c = 5.115(7) Å, and V = 256.7(4) $Å^3$ at room temperature. These values are consistent with those of the synthetic brookite (7): a = 5.4486(3) Å, b = 9.1726(5) Å, c = 5.1361(2) Å, and V = 256.69(2) $Å^3$. The transformation into brookite is of note

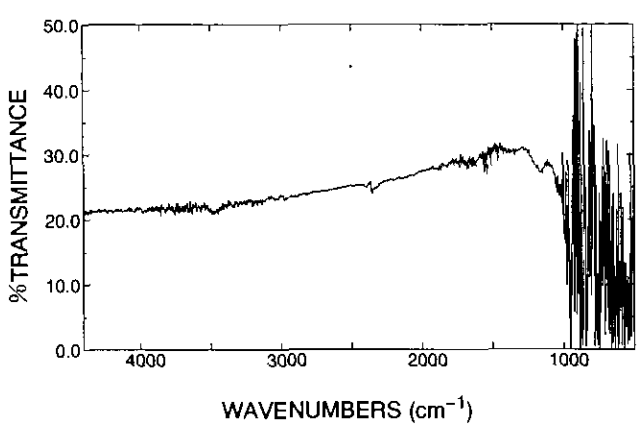

FIG. 4. FT-IR data of TiO_2(R) using a single-crystal specimen.

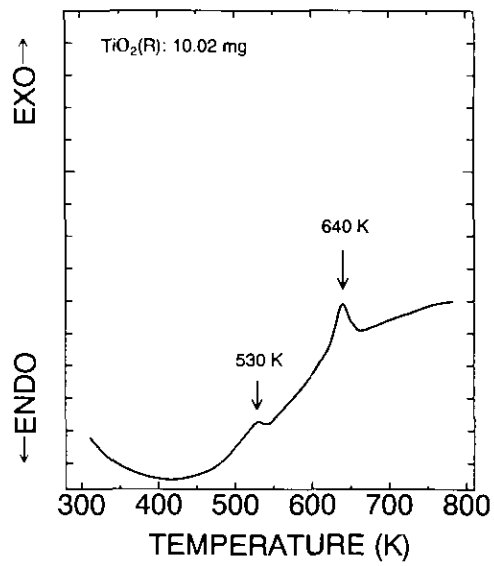

FIG. 5. Differential thermal analysis (10°C/min) of TiO_2(R).

because the other two metastable TiO_2 polymorphs, TiO_2(B) and TiO_2(H), are first transformed into anatase by heating. A precise high-temperature X-ray diffraction study of TiO_2(R) is currently being carried out below and above 640 K.

Single-Crystal X-Ray Diffraction

Precession photographs indicate that all of the crystals, $Li_{0.41}TiO_2$, $Li_{0.16}TiO_2$, $Li_{0.14}TiO_2$, and TiO_2(R), belong to the orthorhombic system with the possible space group $Pbnm$ or $Pbn2_1$, which remains unchanged from that of the as-grown $Li_{0.45}TiO_2$. Figure 6 shows the $\{hk0\}^*$ precession photographs of three specimens: as-grown $Li_{0.45}TiO_2$, $Li_{0.16}TiO_2$, and TiO_2(R). Diffraction patterns of the parent $Li_{0.45}TiO_2$ and of the final product TiO_2(R) are very similar in spot positions but not in intensity for some reflections, e.g., (210), (250), and (310). No further spots indicating the ordered structure could be observed by X-ray diffraction in any of the specimens. For the determination of the lattice parameters of four Li_xTiO_2 crystals, 25 2θ values between 20° and 30° were measured on a Rigaku four-circle diffractometer before and after the intensity data collection using Mo$K\alpha$ radiation. The differences between two pairs of the lattice parameters were within their standard deviations. The final lattice parameters of the four specimens, determined by the least-squares method, are listed in Table 2 together with the data for $Li_{0.45}TiO_2$ (6). The lattice parameters of TiO_2(R) are quite consistent with the results from X-ray powder diffraction (Table 1). Figure 7 shows the approximate linear relations between the lattice parameters and the Li content x in the Li_xTiO_2 composition. Both the a-axis and the b-axis lengths shorten with decreasing Li

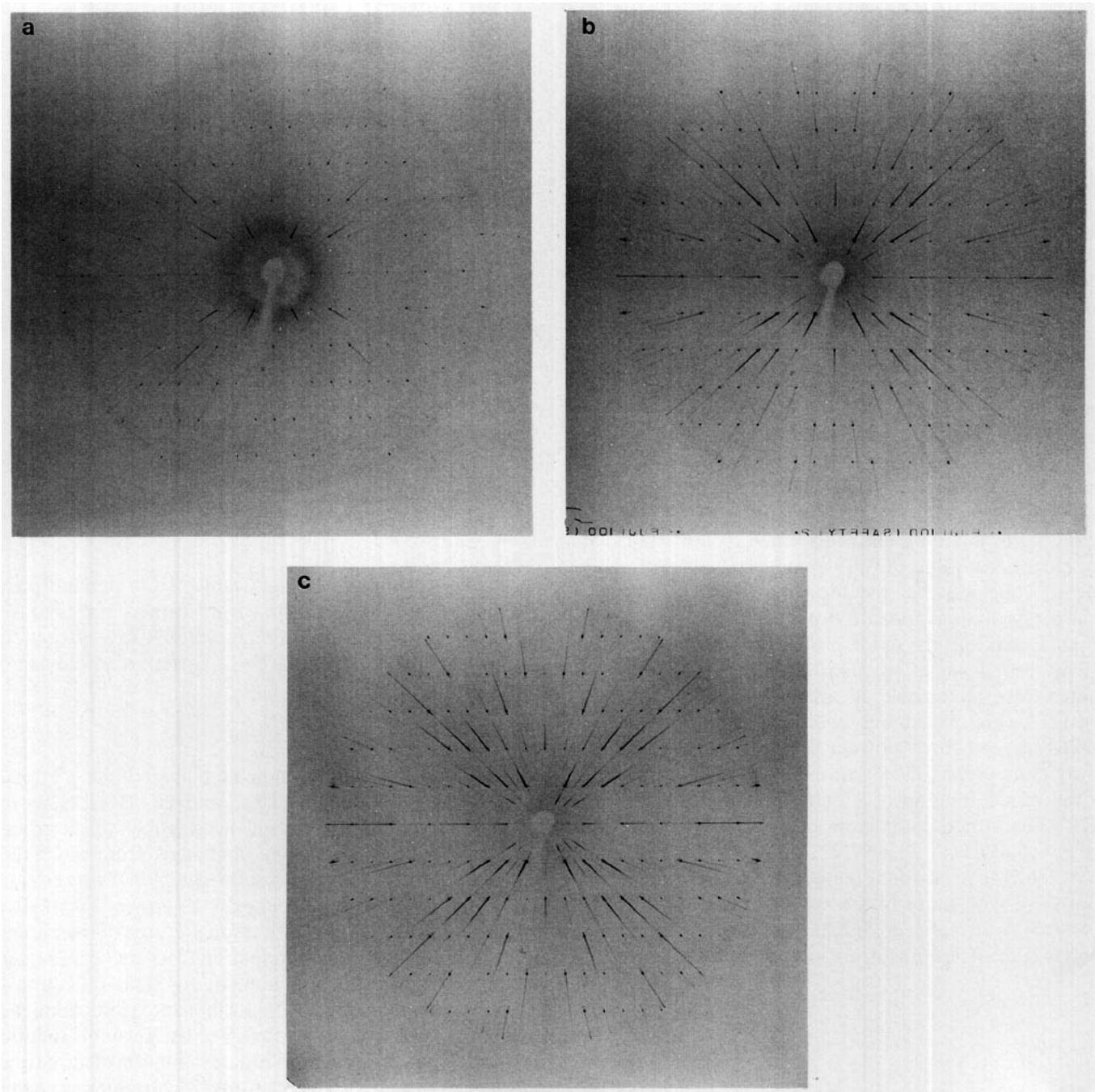

FIG. 6. $\{hk0\}^*$ precession photographs of three Li_xTiO_2 single crystals: (a) as-grown $Li_{0.45}TiO_2$, (b) $Li_{0.16}TiO_2$, and (c) TiO_2(R). Mo$K\alpha$ radiation filtered by Zr foil was used.

content, whereas the c-axis length grows slightly longer. As a result, the unit-cell volume in TiO_2(R) is smaller than that in the parent $Li_{0.45}TiO_2$ by about 6 Å^3, that is, about 4% of the host lattice volume.

Structure Determination

Small block crystals of Li_xTiO_2 (x = 0.41, 0.16, 0.14, and 0) were used for the structure analyses. The intensity data of four ramsdellite-type crystals were obtained under the same experimental conditions used for the $Li_{0.45}TiO_2$ study (6): four-circle diffractometer (operating conditions, 40 kV, 40 mA), graphite-monochromatized Mo$K\alpha$ radiation (λ = 0.71069 Å) in the $2\theta - \omega$ scan mode (maximum 2θ = 100°), scan rate 4°/min, and scan width of 1.0 + 0.5 tan θ at room temperature. Fluctuations of the intensities, monitored by examining a set of three standard reflections

TABLE 2
Crystallographic[a] and Experimental Data for Five Li_xTiO_2 Specimens

	x value[b]				
	0.45[c]	0.41	0.16	0.14	0
Crystal color	Black	Black	Black	Black	Colorless
a (Å)	5.0356(6)	5.0311(9)	4.9794(10)	4.9732(13)	4.9022(14)
b (Å)	9.6377(8)	9.6113(11)	9.5613(13)	9.5425(16)	9.4590(12)
c (Å)	2.9484(7)	2.9488(10)	2.9551(12)	2.9586(16)	2.9585(14)
V (Å^3)	143.09(4)	142.59(6)	140.69(7)	140.41(9)	137.18(7)
Z	4	4	4	4	4
D_x (g/cm^3)	3.85	3.85	3.82	3.83	3.87
D_m (g/cm^3)	—	—	—	—	3.80
Number of observed reflections	845	841	830	829	805
Number of used (>3σ) reflections	744	616	664	671	596
Final R	0.038	0.060	0.048	0.043	0.049
Final wR	0.046	0.050	0.045	0.038	0.044

[a] All compounds belong to the orthorhombic system, space group *Pbnm*.
[b] Determined by the occupancy refinements.
[c] Ref. (6).

((240), (002), (221)) taken after every 50 observations, were within 1.35, 0.88, 1.07, and 1.78% for $Li_{0.41}TiO_2$, $Li_{0.16}TiO_2$, $Li_{0.14}TiO_2$, and TiO_2(R), respectively. The numbers of observed reflections and used reflections are listed in Table 2. No absorption and extinction corrections were performed.

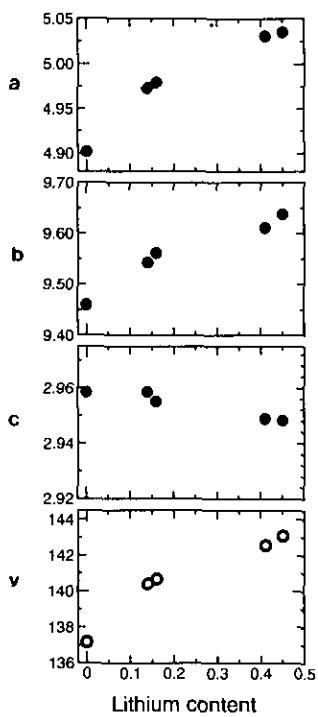

FIG. 7. Lattice parameters a, b, c (Å) and unit-cell volumes V (Å^3) versus Li content x in the Ramsdellite Li_xTiO_2 compounds.

The structure refinements were initiated with the TiO_2 framework using the atomic coordinates in $Li_{0.45}TiO_2$ (6). A full-matrix least-squares refinement using the computer program RFINE-II (8) with anisotropic temperature factors converged to R = 6.6, 5.0, 4.5, and 4.9% for $Li_{0.41}TiO_2$, $Li_{0.16}TiO_2$, $Li_{0.14}TiO_2$, and TiO_2(R), respectively. At this stage, difference-Fourier syntheses using the GSFFR program (9) revealed the occupancy of lithium atoms. Figure 8 shows the z = 1/4 sections of the difference-Fourier maps in the tunnel spaces, together with that of $Li_{0.45}TiO_2$. Decreasing the Li content in Li_xTiO_2 compounds apparently weakens the electron density peak at (−0.05, 0.45, 1/4), and no significant residual peaks are observed in TiO_2(R). No other lithium positions could be observed in the difference-Fourier maps of the Li_xTiO_2 specimens. In the tunnel space of TiO_2(R), the lithium atom with about 5% s.o.f. has been introduced. However, all of the positional parameters, the temperature factor, and the occupancy factor could not be specified, and such a treatment changed the R value and structure factors for the worse. Finally, the lithium site occupancies were refined with anisotropic temperature factors for $Li_{0.41}TiO_2$ and isotropic ones for $Li_{0.16}TiO_2$ and $Li_{0.14}TiO_2$. The site occupancy refinements for Ti in $Li_{0.41}TiO_2$, $Li_{0.16}TiO_2$, $Li_{0.14}TiO_2$, and TiO_2(R) have been applied at the final stages of their refinements, but no evidence that the occupancy factors of Ti should be less than 1.00 could be observed in any of these compounds.

The converged final R values and other crystallographic and experimental data are summarized in Table 2. Difference-Fourier syntheses using the final atomic parameters showed no significant residual peaks. The final atomic coordinates and temperature factors are given in Table

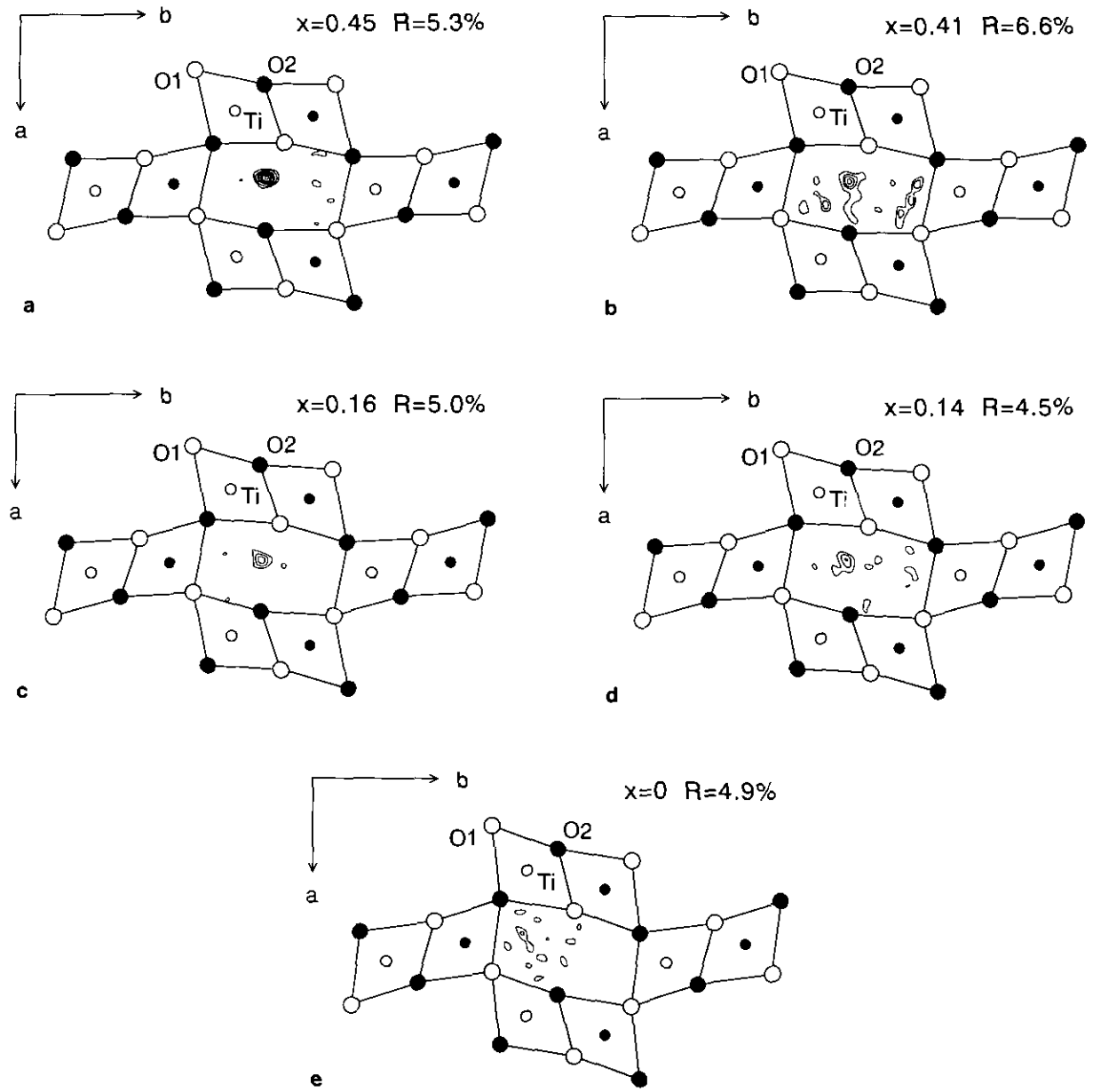

FIG. 8. Difference-Fourier maps at $z = 1/4$, superimposed onto projections of the ramsdellite-type TiO_2 framework viewed down [001], of five Li_xTiO_2 specimens: (a) as-grown $Li_{0.45}TiO_2$, (b) $Li_{0.41}TiO_2$, (c) $Li_{0.16}TiO_2$, (d) $Li_{0.14}TiO_2$, and (e) TiO_2(R). The filled circles represent atoms at $z = 1/4$, and the open circles those at $z = 3/4$. The large circles indicate O, and the small circles Ti atoms. The contour lines are drawn with the interval of 0.6 $e/Å^3$.

3. The scattering factors for the neutral Li, Ti, and O atoms tabulated by Cromer and Mann (10) were used in the calculations. The anomalous dispersion correction factors were taken from the International Tables for X-Ray Crystallography (11).

Crystal Structures of Ramsdellite-Type Li_xTiO_2 ($0 \leq x \leq 0.5$)

The crystal structures of ramsdellite-type $Li_{0.45}TiO_2$ (6), $Li_{0.14}TiO_2$, and TiO_2(R), projected down the c-axis, are drawn with STRUPLO90 (12) in Fig. 9. The selected interatomic distances and bond angles calculated using UMBADTEA (13) are listed in Table 4. The basic framework of the TiO_6 double rutile chain (14) is maintained in the Li_xTiO_2 compounds with $0 \leq x \leq 0.5$. As in the case of the parent $Li_{0.45}TiO_2$ (6), the lithium atoms occupy one tetrahedral site in $Li_{0.41}TiO_2$, $Li_{0.16}TiO_2$, and $Li_{0.14}TiO_2$. The distortion of the LiO_4 tetrahedron in Li_xTiO_2 is scarcely changed from $x = 0.45$ to $x = 0.14$ in spite of the decreasing Li occupancy. The mean Li–O distances

TABLE 3
Atomic Positional Parameters[a] and Anisotropic Temperature Factors[b]

	Li content				
	0.45[c]	0.41	0.16	0.14	0
			Li		
x	−0.057(3)	−0.051(5)	−0.060(10)	−0.066(9)	—
y	0.473(2)	0.467(3)	0.469(5)	0.458(4)	—
β_{11}	0.006(5)	0.002(9)	—	—	—
β_{22}	0.007(2)	0.009(4)	—	—	—
β_{33}	0.08(3)	0.20(7)	—	—	—
β_{12}	0.002(3)	−0.002(4)	—	—	—
B_{eq} or B	1.95	3.49	1.4(9)	1.0(8)	—
s.o.f.	0.45(2)	0.41(3)	0.16(2)	0.14(2)	—
			Ti		
x	−0.01778(10)	−0.02145(16)	−0.03428(16)	−0.03616(12)	−0.06463(17)
y	0.14103(5)	0.14090(8)	0.13918(7)	0.13891(5)	0.13690(7)
β_{11}	0.0051(1)	0.0064(2)	0.0125(2)	0.0131(2)	0.0119(2)
β_{22}	0.00119(3)	0.00092(4)	0.00196(5)	0.00203(4)	0.00186(5)
β_{33}	0.0201(4)	0.0200(6)	0.0226(5)	0.0201(4)	0.0166(5)
β_{12}	0.00016(6)	0.00045(10)	0.00115(10)	0.00111(8)	0.00097(12)
B_{eq}	0.55	0.56	0.92	0.91	0.80
			O(1)		
x	0.7015(4)	0.6962(6)	0.6744(5)	0.6717(4)	0.6365(6)
y	0.2800(2)	0.2784(3)	0.2742(3)	0.2733(2)	0.2663(3)
β_{11}	0.0072(6)	0.0068(9)	0.0076(8)	0.0084(7)	0.0077(8)
β_{22}	0.0019(2)	0.0013(2)	0.0020(2)	0.0021(2)	0.0015(2)
β_{33}	0.018(2)	0.020(3)	0.022(2)	0.019(2)	0.013(2)
β_{12}	0.0020(3)	0.0019(4)	0.0013(3)	0.0014(3)	0.0010(3)
B_{eq}	0.68	0.62	0.75	0.75	0.58
			O(2)		
x	0.2005(4)	0.2007(6)	0.2011(5)	0.2014(4)	0.2084(5)
y	−0.0362(2)	−0.0359(3)	−0.0338(2)	−0.0331(2)	−0.0276(3)
β_{11}	0.0031(5)	0.0032(8)	0.0039(7)	0.0050(5)	0.0055(8)
β_{22}	0.0013(1)	0.0007(2)	0.0015(2)	0.0015(1)	0.0012(2)
β_{33}	0.014(2)	0.020(3)	0.018(2)	0.017(1)	0.012(2)
β_{12}	0.0003(2)	0.0003(3)	0.0002(3)	0.0002(2)	0.0002(3)
B_{eq}	0.42	0.43	0.51	0.54	0.47

[a] All atoms in point position 4c, $\pm(x, y, 1/4)$, $\pm(1/2 - x, 1/2 + y, 3/4)$.
[b] $\beta_{13} = \beta_{23} = 0$.
[c] Ref. (6).

are nearly constant: 2.01–2.02 Å in all of the Li_xTiO_2 compounds. On the other hand, the Li–Li distance along the approximate c-axis direction increases slightly with decreasing Li content (Table 4). This fact can be observed in Fig. 9 as differences in the projections onto the [001] plane of distances between Li (z = 1/4) and Li (z = 3/4) atoms in a tunnel, because the degree of change of the c-axis lengths in these Li_xTiO_2 compounds is very slight. A decrease in the Li content from x = 0.45 to x = 0.14 gradually displaces the lithium atom away from the center of the tunnel (Fig. 9). This may indicate disordered lithium occupation in the tunnel space in the process of topotactic oxidation.

The average octahedral Ti–O distances in the Li_xTiO_2 compounds decrease with decreasing Li content from 1.997 Å in $Li_{0.45}TiO_2$ to 1.973 Å in TiO_2(R), in agreement with the fact that the mean oxidation states of central titanium cations increase from +3.55 to +4.0 (Table 4). With decreasing Li content, Ti–O(1) and Ti–O(2) distances decrease, while Ti–O(1′) and Ti–O(2′) distances slightly increase. Therefore, the O(1)–Ti–O(2′) angle increases from 166.21° in $Li_{0.45}TiO_2$ to 170.57° in TiO_2(R)

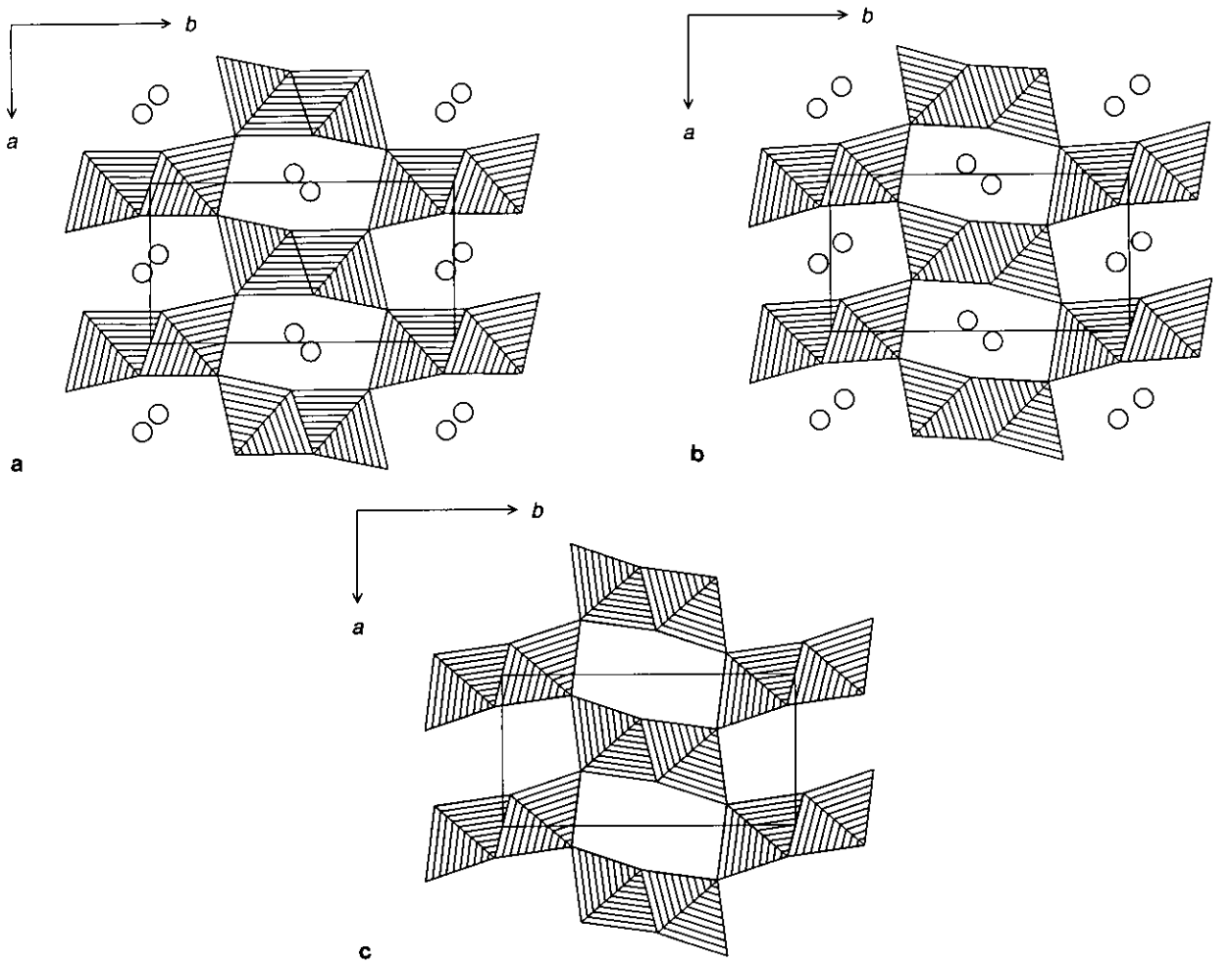

FIG. 9. Crystal structures of Li_xTiO_2 with (a) $x = 0.45$, (b) $x = 0.14$, and (c) TiO_2(R) ($x = 0$). The TiO_6 unit is illustrated as a hatched octahedron. The circles represent Li atoms.

(Table 4). These atomic positional changes with decreasing Li are continuous and can be readily understood by overwritten double rutile chains around the origin of the Li_xTiO_2 compounds with $x = 0.45$, 0.41, 0.16, 0.14, and 0 (Fig. 10). The positional shift of each atom, together with Li content x decreasing from 0.45 to 0, is indicated by arrows in Fig. 10. The degree of shift of the O(2) atom is very slight in comparison with that of the O(1) and Ti atoms. This fact can be explained by the rotation of the double rutile chain. Compared with the double rutile chain in $Li_{0.45}TiO_2$, that in TiO_2(R) rotates slightly around the screw axis parallel to the a-axis, maintaining the ramsdellite framework (Fig. 10). This causes the b-axis length to contract about 0.2 Å, just as a compression of the framework structure along the b-axis would.

Recently, the Li^+/H^+ ion exchange reaction in $Li_2Ti_3O_7$ yielded a new phase, $H_2Ti_3O_7$, with a ramsdellite-type structure. In $H_2Ti_3O_7$ (15), the (Ti, □)O_6 octahedra constructing the ramsdellite framework are less distorted than those in $Li_2Ti_3O_7$ (16, 17) and $Li_{0.45}TiO_2$ (6), and the double rutile chain lies parallel to the b-axis (Fig. 11). Similar framework structures can be seen in the minerals diaspore (α-AlOOH) (18) and groutite (α-MnOOH) (19). This feature is of note because the linkage of the double rutile chain in the present TiO_2(R) is much different from that observed in $H_2Ti_3O_7$ (Fig. 9c). This structural difference between $H_2Ti_3O_7$ and TiO_2(R) is presumed to be mainly determined by the existence of H^+ in the tunnel space.

The hydrogen atoms in $H_2Ti_3O_7$ associated with the O(2) atoms correspond to the longer Ti–O distance. The Ti–O(2) distance in $H_2Ti_3O_7$ (2.018(6) Å) is indeed longer than that in TiO_2(R) (1.937(2) Å), though the Ti–O(2′) distance (2.004(9) Å) is shorter than that in TiO_2(R), the value of which is 2.053(3) Å. On the other hand, the O(2)–O(2) distance, characterizing the possibility of O(2)–H. . .O(2) hydrogen bonding through the tunnel, is 3.015(5) Å in $H_2Ti_3O_7$, which is apparently shorter than the 3.261(5)-Å value in TiO_2(R). In other MOOH com-

TABLE 4
Selected Interatomic Distances (Å) and Bond Angles (°) with Estimated Standard Deviations in Parentheses

	Li content[a]				
	0.45[b]	0.41	0.16	0.14	0
Li–O(1)	2.22(2)	2.22(3)	2.29(5)	2.19(4)	—
Li–O(2)	1.80(2)	1.76(3)	1.79(5)	1.82(4)	—
Li–O(2′) × 2	2.01(1)	2.04(2)	2.00(3)	2.01(3)	—
Mean	2.01	2.02	2.02	2.01	—
Li–Li	1.67(2)	1.68(3)	1.70(5)	1.80(5)	—
O(2)–Li–O(2′)	128.5(5)	128.2(8)	127(1)	124(1)	—
O(2′)–Li–O(2′)	94.4(7)	92(1)	96(2)	95(2)	—
O(2)–Li–O(1)	120.4(9)	124(2)	125(2)	129(2)	—
O(2′)–Li–O(1)	85.5(5)	85.0(9)	85(2)	87(1)	—
Ti–O(1)	1.947(2)	1.940(3)	1.942(3)	1.938(2)	1.909(3)
Ti–O(1′) × 2	1.993(2)	1.994(2)	1.987(2)	1.990(2)	2.000(2)
Ti–O(2) × 2	2.010(1)	2.001(2)	1.972(2)	1.970(1)	1.937(2)
Ti–O(2′)	2.031(2)	2.034(3)	2.027(2)	2.023(2)	2.053(3)
Mean	1.997	1.994	1.981	1.980	1.973
O(1)–Ti–O(1′)	98.02(3)	97.88(4)	96.52(4)	96.36(3)	94.87(4)
O(1)–Ti–O(2)	90.77(7)	90.77(10)	91.43(9)	91.50(7)	93.60(10)
O(1)–Ti–O(2′)	166.21(9)	166.26(13)	166.98(11)	167.16(9)	170.57(11)
O(1′)–Ti–O(1′)	95.42(10)	95.37(14)	96.06(12)	96.06(10)	95.41(12)
O(1′)–Ti–O(2′)	91.23(7)	91.34(10)	92.17(9)	92.21(7)	91.47(9)
O(1′)–Ti–O(2)	84.44(6)	84.20(9)	82.89(8)	82.77(7)	81.89(8)
O(2)–Ti–O(2)	94.34(9)	94.91(13)	97.06(11)	97.31(9)	99.55(12)
O(2)–Ti–O(2′)	79.91(7)	80.00(11)	80.02(9)	80.08(7)	80.37(10)

[a] Determined by the present structure analysis.
[b] Ref. (6).

pounds, the corresponding O–O distances are 2.650(3) Å in diaspore and 2.626 Å in groutite, indicating strong hydrogen bonds. From these structural features, it is confirmed that the tunnel space in TiO_2(R) is truly vacant, as suggested by TGA, IR, and analytical studies.

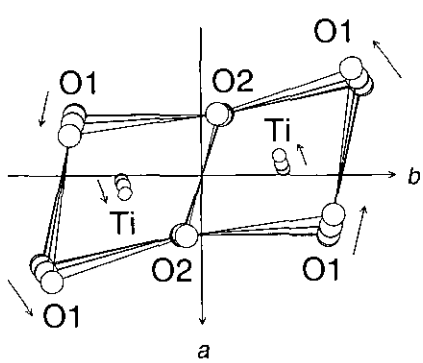

FIG. 10. The continuous change of the double rutile framework with decreasing Li content in Li_xTiO_2. The positional shifts of atoms around the screw axis, together with decreasing Li content, are indicated by arrows.

The accurate chemical composition and crystal structure will be determined by chemical analysis and powder neutron diffraction studies using single-phase polycrystalline samples of Li_xTiO_2 with $0 \leq x \leq 0.5$. The corresponding powder samples have not been prepared yet, because the phase relation between spinel-type $LiTi_2O_4$ and the present ramsdellite-type $Li_{0.5}TiO_2$ is unknown. We are trying to prepare the ramsdellite-type powder samples by a solid-state reaction.

The lattice parameters of some ramsdellite-type titanates are listed in Table 5. It is easy to distinguish

TABLE 5
Lattice Parameters for Some Ramsdellite-Type Titanates

Compound	*a* (Å)	*b* (Å)	*c* (Å)	*V* (Å^3)	Reference
TiO_2(R)	4.9022(14)	9.4590(12)	2.9585(14)	137.18(7)	This study
$Li_{0.5}TiO_2$	5.0356(6)	9.6377(8)	2.9484(7)	143.09(4)	(6)
$Li_2Ti_3O_7$	5.0136(1)	9.5423(1)	2.9438(1)	140.84	(17)
$H_2Ti_3O_7$	4.6745(4)	9.7689(6)	2.9212(2)	133.39(2)	(15)

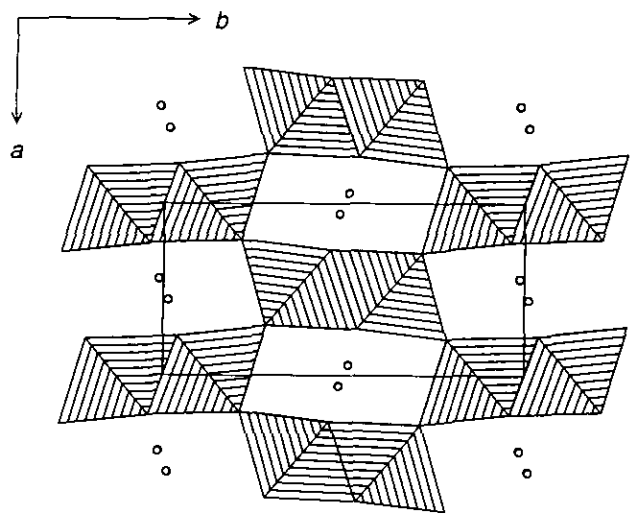

FIG. 11. Crystal structure of $H_2Ti_3O_7$ (15) viewed along [001]. The small circles represent H atoms.

these compounds from each other by the X-ray diffraction method. The lattice parameters of $H_2Ti_3O_7$ are especially different from the other compounds. The differences in *b*-axis length are apparent among these ramsdellite-type titanates, e.g., 9.7689 Å in $H_2Ti_3O_7$, and 9.4590 Å in the present TiO_2(R).

CONCLUSION

The air oxidation of ramsdellite-type $Li_{0.5}TiO_2$ at room temperature allows the preparation of ramsdellite-type bronze crystals having low lithium contents: $Li_{0.41}TiO_2$, $Li_{0.16}TiO_2$, and $Li_{0.14}TiO_2$. The oxidation process together with decreases in both the Li content and the unit-cell volumes was confirmed by a single-crystal X-ray study. Crystals of a new polymorph of titanium dioxide TiO_2(R) were prepared by complete topotactic oxidation using an acidic solution and single crystals of $Li_{0.5}TiO_2$ as a starting material. This form of TiO_2 transforms into brookite when heated above 640 K. The previous two metastable forms, TiO_2(B) and TiO_2(H), have the framework structures of sodium and potassium bronzes, respectively. This new form is based on the host lattice of lithium titanate bronze.

ACKNOWLEDGMENT

The authors are greatly indebted to Dr. I. Nakai, Department of Chemistry, the University of Tsukuba, for his help in density measurements.

REFERENCES

1. R. Marchand, L. Brohan, and M. Tournoux, *Mater. Res. Bull.* **15,** 1129 (1980).
2. S. Andersson and A. D. Wadsley, *Acta Crystallogr.* **15,** 201 (1962).
3. J. F. Banfield, D. R. Veblen, and D. J. Smith, *Am. Miner.* **76,** 343 (1991).
4. J. F. Banfield and D. R. Veblen, *Am. Miner.* **77,** 545 (1992).
5. M. Latroche, L. Brohan, R. Marchand, and M. Tournoux, *J. Solid State Chem.* **81,** 78 (1989).
6. J. Akimoto, Y. Gotoh, M. Sohma, K. Kawaguchi, Y. Oosawa, and H. Takei, *J. Solid State Chem.* **110,** 150 (1994).
7. "Technical Report of National Institute for Research of Inorganic Materials," Vol. 19, p. 44. National Institute for Research of Inorganic Materials, Tsukuba, Japan, 1979.
8. L. W. Finger, "Carnegie Institute of Washington Year Book," Vol. 67, p. 216. Carnegie Institution of Washington, Washington, DC, 1969.
9. M. Ohmasa, "GSFFR: Patterson, Fourier, and Difference Fourier Syntheses Program." 1972.
10. D. T. Cromer and J. B. Mann, *Acta Crystallogr. Sect. A* **24,** 321 (1968).
11. "International Tables for X-Ray Crystallography," Vol. IV, p. 148. Kynoch, Birmingham, 1974.
12. R. X. Fischer, A. le Lirzin, D. Kassner, and B. Rüdinger, *Z. Kristallogr. Suppl. Issue* **3,** 75 (1991).
13. L. W. Finger and E. Prince, "National Bureau of Standards Technical Note," Vol. 854, p. 54. U.S. Government Printing Office, Washington, DC, 1975.
14. A. F. Wells, "Structural Inorganic Chemistry," Fifth ed., p. 219. Oxford Univ. Press, New York, 1984.
15. A. le Bail and J. L. Fourquet, *Mater. Res. Bull.* **27,** 75 (1992).
16. B. Morosin and J. C. Mikkelsen, Jr., *Acta Crystallogr. Sect. B* **35,** 798 (1979).
17. I. Abrahams, P. G. Bruce, W. I. F. David, and A. R. West, *J. Solid State Chem.* **78,** 170 (1989).
18. W. R. Busing and H. A. Levy, *Acta Crystallogr.* **11,** 798 (1958).
19. L. S. D. Glasser and L. Ingram, *Acta Crystallogr. Sect. B* **24,** 1233 (1968).